Postprint of: Ullah U., Kozieł S., Mabrouk I., A Simple-Topology Compact Broadband Circularly Polarized Antenna With Unidirectional Radiation Pattern, IEEE Antennas and Wireless Propagation Letters, Vol. 18, iss. 12 (2019), pp. 2612-2616, DOI: 10.1109/LAWP.2019.2945543

A Simple-Topology Compact Broadband Circularly Polarized Antenna With Unidirectional Radiation Pattern

Ubaid Ullah, Slawomir Koziel, *Senior Member, IEEE*, and Ismail Ben Mabrouk

***Abstract*—In this letter, a geometrically simple, reflector-backed single-point-fed circularly polarized (CP) antenna with unidirectional radiation pattern is presented. The structure comprises a simple coplanar waveguide (CPW) feeding circuit with an open slot etched on one side of the coplanar ground. The enhanced CP bandwidth is obtained by combining the loop mode, the slot mode, and the asymmetrical configuration of the coplanar ground planes along the feed line. All parameters are optimized at the full-wave level of description for the best impedance and axial ratio (AR) bandwidth. The antenna footprint is only 0.35 λ_o × 0.39 λ_o at the lowest CP operating frequency of 3.1 GHz. The measurement results indicate 82% impedance bandwidth (from 3 GHz to 7.2 GHz), and 80% AR bandwidth (from 3.1 GHz to 7.2 GHz). A unidirectional right-hand circular polarization (RHCP) radiation pattern in the +*z*-direction is also achieved by adding a reflector. The peak realized gain of the antenna is 6.7 dBic, and the peak radiation efficiency is 98%.**

***Index Terms*—Wideband antennas, compact antennas, wide slot antenna, EM-driven design, circularly polarized antenna.**

I. Introduction

Circularly polarized (CP) antennas are highly attractive for modern wireless communication systems. Circular polarization allows for reducing the multipath effects, polarization mismatches and Faraday's rotation effects in the ionosphere [1-3]. Due to these features, CP antennas achieves a stable communication link between the transmitter and receiver [4]. Implementation-wise, CP radiation can be realized by modifying conventional radiators (e.g., through multi-point feeding [5]), yet typically at the expense of topological complexity and increased physical size [6].

To comply with the bandwidth requirements of the wireless communication systems, printed wide-slot type antennas have been proposed [6-13]. Circular polarization can be induced in these antennas by simple topological modifications [9-11]. Furthermore, multiple CP operating modes at different frequencies can be merged together to enhance the impedance bandwidth and the AR bandwidth [13-14]. Other properties of wide-slot antennas include low cost, low profile, ease of integration, compact size, and simple feeding [15].

The literature offers a wide variety of bi-directional wide-slot antennas [6]-[11], yet CP structures with unidirectional radiation characteristics are of particular interest [16]. Maintaining a broadband operation and a unidirectional radiation pattern is challenging. Although this can be achieved with cross dipole antennas, they require additional circuit components, such as, couplers, which increases the complexity of the feeding circuit and the transmission line losses [17]. This is not necessary in the case of wide-slot structures, which can also be easily manipulated to alter their field characteristics. Examples include adding a reflector to realize a unidirectional radiation pattern [18], [19]. Unfortunately, this is normally associated with a complex feeding structure or incorporating additional components necessary to ensure broadband operation [19] [24].

In this letter, a simple configuration of the planar wide-slot antenna featuring broadband CP operation and unidirectional radiation characteristics is presented. The antenna employs a single-point CPW-fed open slot configuration etched on one side of the coplanar ground plane. The broadband impedance and AR bandwidth is achieved by merging the three resonant modes induced by: The asymmetrical ground planes along the length of the microstrip line, the modified geometry of the wide-slot and the loop formed within the slot. A flat reflector is used to render a unidirectional radiation pattern. The measured impedance bandwidth is 82% (3 GHz to 7.2 GHz) and the axial ratio (AR) bandwidth is 80% (3.1 GHz to 7.2 GHz), which gives 98% bandwidth overlap between S_{11} and AR. The peak realized gain of the antenna is 6.7 dBic and the peak radiation efficiency is 98%. The structure is suitable for C-band, 3.3 GHz, 3.5 GHz and 5.5 GHz WiMax, as well as 5.2 GHz and 5.8 GHz WLAN applications.

The novel components of the work include: (i) design of a low cost, single-point-fed unidirectional CP antenna; (ii) achieving broadband characteristics by combining multiple CP modes generated through a modified slot shape; (iii) ensuring topological simplicity of the design; (iv) rigorous parametric optimization resulting in excellent performance, especially low levels of axial ratio.

Manuscript submitted on July 3, 2019. This work was supported in part by the ADEK Award for Research Excellence (AARE) 2018, Abu Dhabi, United Arab Emirates, Under Project AARE18-203, Icelandic Centre for Research (RANNIS) Grant 174114051, and by the National Science Centre of Poland Grant 2017/27/B/ST7/00563.

U.Ullah and Ismail Mabrouk are with Networks and Communication Engineering department, Al Ain university of Science and Technology, P.O.Box (112612), Abu Dhabi, UAE. (ubaid.ullah@aau.ac.ae, ismail.mabrouk@aau.ac.ae)

S. Koziel is with Engineering Optimization and Modeling Center of Reykjavik University, Reykjavik, Iceland; S. Koziel is also with the Faculty of Electronics, Telecommunications and Informatics, Gdansk University of Technology, 80-233 Gdansk, Poland (e-mail: koziel@ru.is).

This article has been accepted for publication in a future issue of this journal, but has not been fully edited. Content may change prior to final publication. Citation information: DOI 10.1109/LAWP.2019.2945543, IEEE Antennas and Wireless Propagation Letters

II. Antenna Design And Configuration analysis

The parameterized geometry of the proposed antenna is shown in Fig. 1. The values of its geometry parameters are listed in the caption. The design is implemented on a laminated Rogers RO4003C substrate (ε_r = 3.38, tanδ = 0.0027, h = 0.813 mm) with the external dimensions $L_s \times W_s$. The antenna structure employs a coplanar waveguide (CPW) feeding line printed on the top layer of the substrate. The 50 Ohm CPW excitation is designed with the coplanar gap g = 0.6325, length L_m and width W_m of the microstrip line. A wide slot is etched on the left-hand-side of the transmission line, and the coplanar ground planes are made asymmetric along the line length in the y-direction. This configuration leads to a broadband response in terms of the impedance bandwidth and the AR bandwidth. The development stages of the proposed antenna and its operation mechanism are further explained in the following sections.

A. Antenna Development

The antenna development stages are shown in Fig. 2. At the first stage, the asymmetrical design of the CPW is printed on the substrate with a straight microstrip line monopole extension. The length of the microstrip monopole is 25.05 mm which is approximately a quarter wavelength at the lower cut-off frequency and half a wavelength near the CP center operating frequency. Figure 3 shows the relevant antenna characteristics corresponding to the stages of Fig. 2. The S_{11} response at Stage 1 shows a resonance near the center frequency with an overall poor impedance matching. The AR response shows that the antenna is somewhat circularly polarized which is attributed to the asymmetrical topology of the CPW.

At the second stage, a rectangular slot is formed within the coplanar ground plane to the left of the transmission line. This creates an additional current path along x and y-direction. The impedance matching at this stage shows a clear improvement which also leads to the enhancement of the impedance bandwidth. Consequently, the antenna Q-factor which is the measure of the antenna impedance bandwidth relative to its center frequency is lowered. Moreover, the AR response related to Stage 2 (Fig. 3(b)) is also improved which is due to the induction of the additional electric (E) field component along W_{s2} and L_{s2} (See Fig.1 (a)). The antenna reflection coefficient shows a resonance at 3 GHz and above 5 GHz, whereas the 4 GHz region is still well above –10 dB. Also, there is a narrow AR bandwidth at the lower end of the antenna operating band which is due to the current flowing along L_{s2}, W_{s2}, and Ls_3 forming a partial loop. The surface current distribution for the loop current is shown in Fig. 2(b).

In Stage 3, the current path is lengthened by extending the slot in the –y-direction; also a stub is protruded along the length of the CPW feedline. Upon the initial sizing of the antenna structure, an acceptable broadband response in terms of S_{11} and AR is achieved from 3 GHz to 7 GHz. Subsequently, all the antenna parameters are optimized at the full-wave EM level of description. The goal is the improvement of both S_{11} and AR. The optimized results are shown in Fig. 3 as the Stage 3 results. Note that the antenna at this stage is operating with bidirectional radiation characteristics and the peak realized gain of 3.17 dBic.

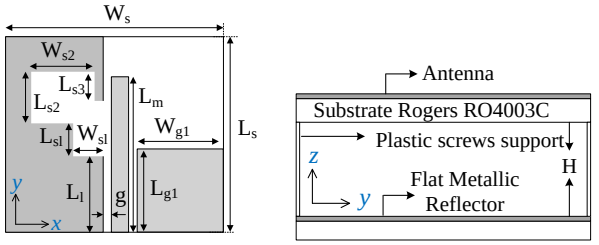

Fig. 1. Geometrical configuration of the proposed broadband unidirectional CP antenna: (a) top view (b) side view (L_s=33.5, L_{s1}=7.3, L_{s2}=10.49, W_s=37.6, W_{s1}=3.9, W_{s2}=7.48, L_{s1}=14.52, L_m=25.05, g=0.6325, W_{g1}=17.81, W_m=1.35, L_{s3}=4.73, L_1=10.76, H=18.98, all values in millimeter (mm))

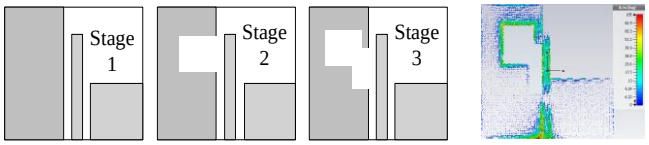

Fig. 2. Antenna design stages and the surface current: (a) stages 1 through 3, (b) loop current around the lower end of the operating band (4 GHz).

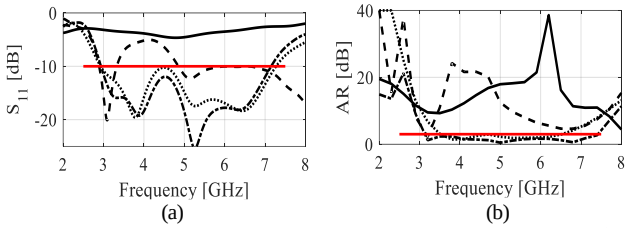

Fig. 3. Antenna characteristics through the evolution stages: Stage 1 (——), Stage 2 (----), Stage 3 (….), and Stage 4 (- · - · -): (a) $|S_{11}|$, (b) AR.

To make the antenna unidirectional, a flat reflector of the same size as that of the antenna itself is placed at a distance H as shown in Fig 1(b). All antenna parameters, including H, are optimized again and the results are plotted in Fig. 3 and represented as Stage 4 results. The simulation at this stage indicates a broadband CP characteristic from 3.1 GHz to 7.2 GHz with the peak realized gain of 6.7 dBic.

B. Parametric Analysis and Antenna Operating Mechanism

In order to explain the antenna operating mechanism and the effects of the structure parameters on the antenna performance figures, a detailed parametric study is carried out. The results are shown in Fig. 4. Varying the value of L_{g2} indicates that the antenna impedance matching is affected by this parameter, although the antenna retains its operating bandwidth from 3 GHz to 7.2 GHz. This parameter also has a slight effect on the antenna AR near the 3.6 GHz. Parameter L_{s1} plays an important role in expanding both the antenna impedance bandwidth and the AR bandwidth. By reducing L_{s1}, the impedance bandwidth and AR improves, especially at the upper frequencies, but the AR near the lower frequency starts violating the 3 dB criterion. The analysis of W_{s1} shows that by increasing its value, the upper cut-off frequency can be controlled both in terms of S_{11} and AR. Note that L_{s1} and W_{s1} are the length and the width of the rectangular slot extension in the –y-direction. The length and the width of the larger portion of the slot is defined by L_{s2} and W_{s2}, respectively. Varying L_{s2} allows us to control the impedance matching, whereas the width W_{s2} tunes the lower

This article has been accepted for publication in a future issue of this journal, but has not been fully edited. Content may change prior to final publication. Citation information: DOI 10.1109/LAWP.2019.2945543, IEEE Antennas and Wireless Propagation Letters

cut-off frequency. Moreover, by changing W_{s2}, AR at the lower frequency can be adjusted as well. The parameter L_{s3} controls the impedance matching at the lower edge with almost negligible effect on the AR. The operating mechanism is explained based on the electric field distribution on the antenna at 3.5 GHz, 5 GHz, and 6.5 GHz. At 3.5 GHz, the high-intensity current is mainly distributed at the surrounding of the slot as depicted in Fig. 6(a). For the loop mode shown in Fig. 6(b) at 5 GHz, the current distribution is visibly high at the edges of the open slot. Finally, the current distribution at the monopole and the right-side ground plane is shown at 6.5 GHz (Fig. 6(c)). The current intensities indicate that the CP is induced by the monopole and the right-hand-side ground plane. The theoretical explanation of the loop mode and the slot mode for the printed slot type antennas presented in [13] apply to the structure presented here.

C. *Reflector Distance Effect on Realized Gain*

The effect of the reflector distance H on the realized gain of the antenna is studied here. The realized gain shown in Fig. 5 (a) is evaluated for $H = 0.25\lambda$ at the 3.5 GHz, 5 GHz and 7 GHz.

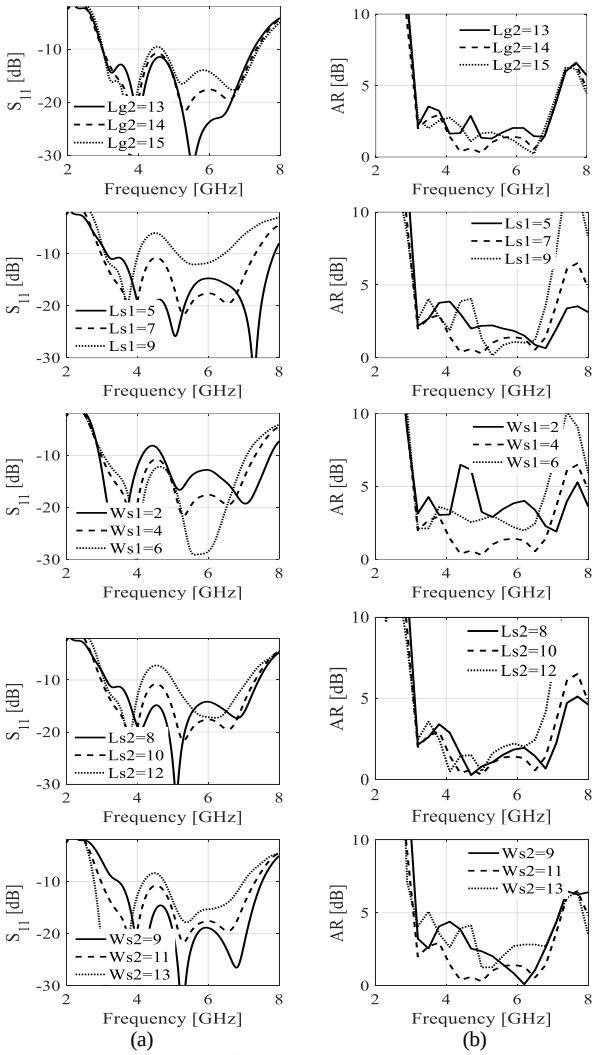

Fig. 4. Parametric analysis of the antenna electrical characteristics: (a) $|S_{11}|$, (b) AR.

When $H = 0.25\lambda$ at 3.5 GHz, maximum AR bandwidth of 80% is achieved. For 5 GHz and 7 GHz, the AR bandwidth is 57% (3.6 GHz to 6.5 GHz) and 40% (4 GHz to 6 GHz), respectively. Due to the broadband nature of the antenna, a constant distance of 0.25λ cannot be maintained for all frequencies which leads to destructive interference and hence the realized gain drop at certain frequencies. In this work compromise between the realized gain and the AR bandwidth is made and $H = 0.25\lambda$ near 3.5 GHz is used. The effect of the reflector distance on S_{11} and AR is also shown in Fig. 5(b) and Fig. 5(c), respectively. A monotonic relationship between the antenna-to-reflector distance and the AR bandwidth can be observed.

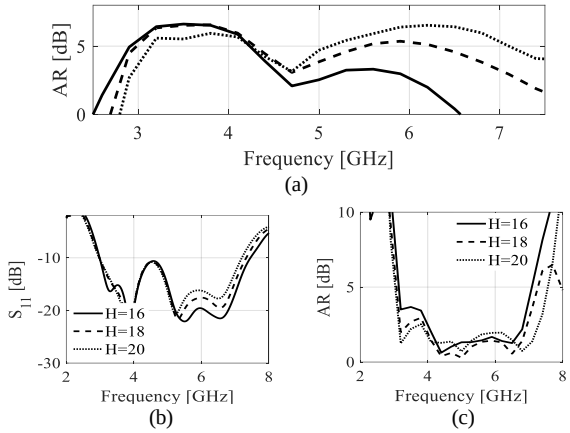

Fig. 5. The effect of reflector distance H: (a) Realized gain $H = 0.25\lambda$ at: 3.5 GHz (——), 5GHz (----), and 7 GHz (….), (b) $|S_{11}|$, (c) AR

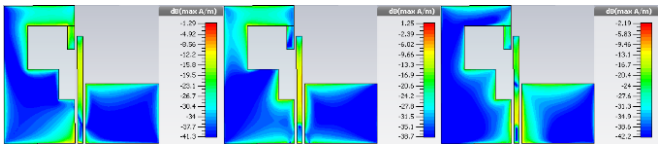

Fig. 6. Antenna electric field at three different frequencies (a) 3.5 GHz (b) 5GHz, (c) 6.5 GHz

III. Experimental Validation

A prototype of the proposed unidirectional CP antenna is fabricated as shown in Fig. 6, and validated experimentally. A broad impedance bandwidth and AR bandwidth have been achieved with a close agreement between the simulation and the measurement. The S_{11} and AR characteristics shown in Fig. 8 indicate an impedance bandwidth $|S_{11}| > -10$ dB of 82% from 3 GHz to 7.2 GHz and the AR bandwidth of 80% from 3.1 GHz to 7.2 GHz. The simulated and measured realized gain of the antenna is depicted in Fig. 9(a). The peak realized gain (both simulated and measured) is approximately 6.7 dBic. The realized gain can be easily improved and stabilized by using a larger size cavity instead of the flat reflector. The simulated and measured efficiencies of the antenna are depicted in Fig. 9(b). The peak radiation efficiency of the antenna is 98% while the maximum total efficiency of 94% is recorded. The radiation pattern of the proposed antenna is also measured in both the *xz*- and the *yz*-planes at 3.5 GHz, 4.5 GHz, 5.5 GHz, and 6.5 GHz. Figure 10 shows the radiation pattern in the *xz*-plane with a relatively stable

This article has been accepted for publication in a future issue of this journal, but has not been fully edited. Content may change prior to final publication. Citation information: DOI 10.1109/LAWP.2019.2945543, IEEE Antennas and Wireless Propagation Letters

radiation pattern in the +*z*-direction. Similarly, the *yz*-plane pattern is also measured and depicted in Fig. 11. The slight beam tilt at some frequencies is due to the asymmetric configuration of the CPW. For both planes, a unidirectional right-hand circular polarized (RHCP) patterns are obtained. At 6.5 GHz the LHCP is slightly higher but away from the main beam direction and the antenna still maintains an acceptable radiation pattern in the $\theta = 0$ direction. The cross-pol level can be further improved by reducing the reflector height but, as mentioned in Section II.*B*, the reflector height is kept to a quarter wavelength to ensure wider AR bandwidth. In other words, the obtained design is a trade-off between the AR bandwidth and other performance figures (specifically, cross-polarization level), here, inclined towards the high quality of circular polarization. The antenna without the reflector operated in a bidirectional manner with RHCP in the +*z*-direction and LHCP in the –*z*-direction.

For benchmarking, the proposed antenna is compared with the recent state-of-the-art unidirectional designs in terms of the AR bandwidth and the total footprint in Table I.

(a) (b)

Fig. 7. Photographs of the fabricated antenna prototype: (a) front view, (b) 3D view.

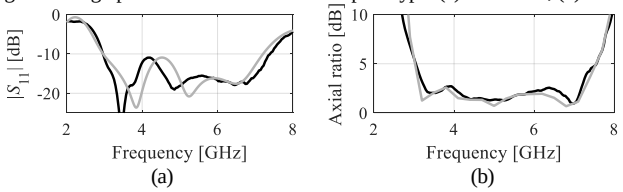

(a) (b)

Fig. 8. Simulated (gray) and measured (black) characteristics of the antenna prototype: (a) reflection, (b) axial ratio in a broadside direction.

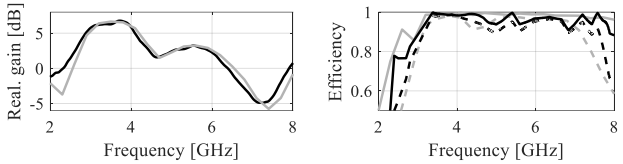

Fig. 9. Simulated (gray) and measured (black) realized gain of the proposed antenna in a broadside direction, and its efficiencies (total – dashed line, radiation – solid line).

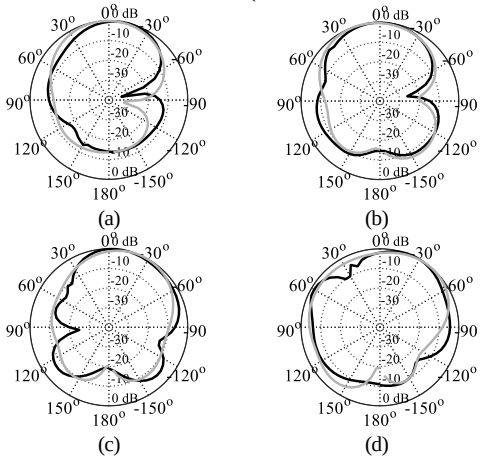

(a) (b) (c) (d)

Fig. 10. Simulated (gray) and measured (black) radiation patterns of the proposed antenna in the xz-plane: (a) 3.5 GHz, (b) 4.5 GHz, (c) 5.5 GHz, (d) 6.5 GHz. RHCP and LHCP shown using solid and dashed lines, respectively.

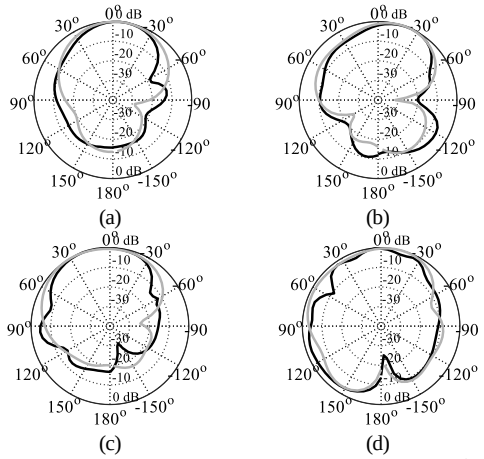

(a) (b) (c) (d)

Fig. 11. Simulated (gray) and measured (black) radiation patterns of the proposed antenna in the *yz*-plane: (a) 3.5 GHz, (b) 4.5 GHz, (c) 5.5 GHz, (d) 6.5 GHz. RHCP and LHCP shown using solid and dashed lines, respectively.

TABLE I COMPARISON WITH STATE-OF-THE-ART CP ANTENNAS

Ref	%AR	%BW	Overall Size [λ_o]	Substrate (h (mm), ε)
[14]	53.4	67.4	1.1×1.1×0.28	F4B-2(0.8,2.65)
[15]	60.9	110	0.92×0.92×0.31	FR4 (1,4.4)
[16]	27	50.2	0.48×0.48×0.24	FR4 (1.6,4.4)
[17]	50	71	0.58×0.58×0.23	(1,2.65)
[18]	53	….	1.88×1.13×0.30	FR4 (1.6,4.4)
[20]	58.6	68.9	0.79×0.79×0.27	RT(0.81, 3.38)
[21]	51	57	0.88×0.88×0.23	RT(0.81, 3.38)
[22]	26.8	59.77	0.64×0.64×0.16	RT(0.81, 3.38)
[23]	74.1	91.4	1.01×1.01×0.29	F4B(0.8,2.65)
Proposed	81	89	0.58×0.65×0.32	RT(0.81, 3.38)

The antenna size is calculated with respect to the CP center frequency. It can be observed that the proposed antenna features a broad AR bandwidth and the smallest footprint compared to most of the benchmark designs. The designs presented in [16] and [17] feature smaller sizes but both are inferior to the proposed design in terms of S_{11} and AR. The advantage of this design is that the broadband characteristics have been achieved with a simple topology, compact size and without involving any external active components.

IV. CONCLUSION

A broadband unidirectional CP antenna with a simple geometry has been presented. The proposed antenna comprises an asymmetrical CPW and an inverted L-shape open slot/loop created in one of the coplanar ground planes. The broadband response in terms of impedance bandwidth and the AR bandwidth has been achieved by combining the slot mode, the loop mode and the microstrip line monopole with the asymmetrical ground plane. The structure is fully optimized before prototyping and experimental characterization. A compact geometry of the radiator (0.35 λ_o × 0.39 λ_o), broad impedance bandwidth of 82%, AR bandwidth of 80%, and peak realized gain of 6.7 dBic has been achieved with the RHCP radiation pattern in the +*z*-direction. The peak radiated and total efficiencies of the antenna is 98% and 94% respectively.

This article has been accepted for publication in a future issue of this journal, but has not been fully edited. Content may change prior to final publication. Citation information: DOI 10.1109/LAWP.2019.2945543, IEEE Antennas and Wireless Propagation Letters

REFERENCES

[1] E. Arnieri, L. Boccia, G. Amendola, and G. D. Massa, "A compact high gain antenna for small satellite applications," *IEEE Trans. Antennas Propag*., vol. 55, no. 2, pp. 277–282, Feb. 2007.

[2] M. Shokri, V. Rafii, S. Karamzadeh, Z. Amiri, and B. Virdee, "Miniaturized ultra-wideband circularly polarised antenna with modified ground plane," *Electron. Lett*., vol. 50, no. 24, pp. 1786–1788, 2014.

[3] U. Ullah and S. Koziel, "Design and optimization of a novel miniaturized low-profile circularly polarized wide-slot antenna," *Journal of Electromagnetic Waves and Applications*, vol. 32, no.16, pp. 2099–2109, 2018.

[4] K. O. Gyasi, G. Wen, D. Inserra, Y. Huang, J. Li, A. E. Ampoma , and H. Zhang, "A compact broadband cross-shaped circularly polarized planar monopole antenna with a ground plane extension," *IEEE Antennas Wireless Propag. Lett*., vol. 17, no. 2, pp. 335–338, 2018.

[5] U. Ullah, M. F. Ain, and Z. A. Ahmad, "A review of wideband circularly polarized dielectric resonator antennas," *China Commun.*, vol. 14, no. 6, pp. 65–79, 2017.

[6] Y.-M. Cai, K. Li, Y.-Z. Yin, and W. Hu, "Broadband circularly polarized printed antenna with branched microstrip feed," *IEEE Antennas Wireless Propag. Lett*., vol. 13, pp. 674–677, 2014.

[7] T. Kumar and A. R. Harish, "Broadband circularly polarized printed slot-monopole antenna," *IEEE Antennas Wireless Propag. Lett*., vol. 12, pp. 1531–1534, 2013.

[8] R. C. Han, and S.-S. Zhong, "Broadband circularly-polarised chifreshaped monopole antenna with asymmetric feed," *Electron. Lett*., vol. 52, no. 4, pp. 256–258, Feb. 2016.

[9] U. Ullah and S. Koziel, "Design and optimization of a novel compact broadband linearly/circularly polarized wide-slot antenna for wlan and WiMAX applications," *Radioengineering.*, vol. 27, no 1, pp. 19–24, 2019

[10] C. Wang, M. Shih, and L. Chen, "A wideband open-slot antenna with dual-band circular polarization," *IEEE Antennas Wireless Propag. Lett.*, vol. 14, pp. 1306–1309, 2015.

[11] U. Ullah and S. Koziel, "A broadband circularly polarized wide-slot antenna with a miniaturized footprint," *IEEE Antennas Wireless Propag. Lett.*, vol. 17, no. 12, pp. 2454–2458, 2018.

[12] X. Ding, Z. Zhao, Y. Yang, Z. Nie and Q. H. Liu, "A compact unidirectional ultra-wideband circularly polarized antenna based on crossed tapered slot radiation elements," *IEEE Trans. Antennas Propag*, vol. 66, no. 12, pp. 7353-7358, Dec. 2018.

[13] G. Pan, Y. Li, Z. Zhang and Z. Feng, "A compact wideband slot-loop hybrid antenna with a monopole feed," *IEEE Trans. Antennas Propag*, vol. 62, no. 7, pp. 3864-3868, July 2014.

[14] G. Feng, L. Chen, X. Xue, and X. Shi, "Broadband circularly polarized crossed-dipole antenna with a single asymmetrical cross-loop," *IEEE Antennas Wireless Propag. Lett*., vol. 16, pp. 3184–3187, 2017

[15] G. Li, H. Zhai, L. Li and C. Liang, "A nesting-L slot antenna with enhanced circularly polarized bandwidth and radiation," *IEEE Antennas Wireless Propag. Lett*, vol. 13, pp. 225-228, 2014.

[16] Y. He, W. He, and H. Wong, "A wideband circularly polarized cross-dipole antenna," *IEEE Antennas and Wireless Propag. Lett*., vol. 13, pp. 67–70, 2014.

[17] J. Wei, X. Jiang and L. Peng, "Ultrawideband and high-gain circularly polarized antenna with double-y-shape slot," *IEEE Antennas and Wireless Propagation Letters*, vol. 16, pp. 1508-1511, 2017.

[18] J. Chen and J. Row, "Wideband circularly polarized slotted-patch antenna with a reflector," *IEEE Antennas and Wireless Propag. Lett*, vol. 14, pp. 575-578, 2015.

[19] H. H. Tran, I Park, and T. K. Nguyen, "Circularly polarized bandwidthenhanced crossed dipole antenna with a simple single parasitic element," IEEE Antennas Wireless Propag. Lett., vol. 16, pp. 1776–1779, 2017

[20] H. H. Tran, I. Park and T. K. Nguyen, "Circularly polarized bandwidth-enhanced crossed dipole antenna with a simple single parasitic element," *IEEE Antennas and Wireless Propag. Lett*, vol. 16, pp. 1776-1779, 2017.

[21] H. H. Tran and I. Park, "Wideband circularly polarized cavity-backed asymmetric crossed bowtie dipole antenna," *IEEE Antennas Wireless Propag. Lett*, vol. 15, pp. 358-361, 2016.

[22] S. X. Ta and I. Park, "Crossed dipole loaded with magneto-electric dipole for wideband and wide-beam circularly polarized radiation," *IEEE Antennas Wireless Propag. Lett*, vol. 14, pp. 358-361, 2015.

[23] Y. Li, Z. Zhao, J. Liu, and Y.-Z. Yin, "A cavity-backed wideband circularly polarized crossed bowtie dipole antenna with sequentially rotated parasitic elements," *Progress in Electromagnetics Research Letters*, vol. 79, pp. 1-7, 2018.

[24] J. Pourahmadazar, C. Ghobadi, J. Nourinia, N. Felegari and H. Shirzad, "Broadband CPW-fed circularly polarized square slot antenna with inverted-L strips for UWB applications," *IEEE Ant. Wireless Prop. Lett.*, vol. 10, pp. 369-372, 2011.